Physica E 61 (2014) 118–124

Contents lists available at ScienceDirect

Physica E

journal homepage: www.elsevier.com/locate/physe

Transport in graphene nanostructures with spatially modulated gap and potential

E.S. Azarova, G.M. Maksimova *

Department of Theoretical Physics, University of Nizhny Novgorod, 23 Gagarin Avenue, 603950 Nizhny Novgorod, Russian Federation

HIGHLIGHTS

- Resonant-peak positions do not depend on the number of barriers at certain conditions.
- Gapped fractions cause decrease (increase) of the conductance (Fano factor).
- Gapped-graphene regions affect the Fano factor stronger than the conductivity.

ARTICLE INFO

Article history:
Received 28 January 2014
Received in revised form
21 March 2014
Accepted 25 March 2014
Available online 2 April 2014

Keywords:
Graphene superlattice
Conductance
Shot noise
Dirac points

ABSTRACT

We study transport properties of graphene nanostructures consisted of alternating slabs of gapless ($\Delta = 0$) and gapped ($\Delta \neq 0$) graphene in the presence of piecewise constant external potential equal to zero in the gapless regions. The transmission through single-, double-barrier structures and superlattices has been studied. It was revealed that any n-barrier structure is perfectly transparent at certain conditions defining the positions of new Dirac points created in the superlattice. The conductance and the shot noise were as well computed and investigated for the considered graphene systems. In a general case, the existence of gapped graphene fraction leads to a decrease of the conductance and an increase of the Fano factor. For two barriers formed by gapped graphene and separated by a long and highly doped region the Fano factor rises up to 0.5 in contrast to a similar gapless structure where the Fano factor is close to 0.25. Similar to a gapless graphene superlattice, creation of each new Dirac point manifests itself as a conductivity resonance and a narrow dip in the Fano factor. However, gapped graphene inclusion into the potential-barrier regions in the superlattice leads to more complicated dependence of the Fano factor on the potential height compared to pseudo-diffusive behavior (with $F=1/3$) typical for a gapless superlattice.

1. Introduction

Transport properties of graphene and graphene-based microstructures are currently among the most actively investigated topics in graphene physics [1–11]. Aside from fundamental aspects such interest in graphene stems from its potential applications as a high-mobility semiconductor and the experimental ability to tune its properties via gating [2]. Investigation of the electron transport includes the consideration of a conductance and shot noise which is characterized by the Fano factor F being the ratio of the noise power and mean current. For instance, the Fano factor of wide and short graphene sheet equals 1/3 [6] near the Dirac point. This coincides with the well-known result for diffusive wire [12].

Lots of theoretical and experimental works have been devoted to investigations of transmission T and conductance G through different multibarrier graphene nanostructures and graphene superlattices (SLs) [13–23] which can be fabricated, e.g., by applying a local top gate voltage. It has been shown that a one-dimensional periodic potential substantially affects the transport properties of graphene. For instance, the Kronig–Penney type electrostatic potential produces strong anisotropy in the carrier group velocity near the Dirac point leading to the supercollimation phenomenon [24–26].

The band structure of an ideal graphene sheet has no energy gap which results, for example, in total transparency of any potential barrier for normally incident electrons [27] (an analog of the Klein paradox [28]). It is extremely desirable for electronics applications that graphene structures be gapped. Therefore, much effort of researchers has been focused on producing a gap in the graphene spectrum. The gap can be created by strain engineering as well as by deposition or adsorption of molecules on a graphene

* Corresponding author. Tel.: +7 831 4623304.
E-mail address: maksimova.galina@mail.ru (G.M. Maksimova).

http://dx.doi.org/10.1016/j.physe.2014.03.023
1386-9477/

layer. For instance, a hydrogenated sheet of graphene (graphane) is a semiconductor with a gap of the order of a few eV [29]. Other way of producing the gap is to use a hexagonal boron nitride (hBN) substrate. In this case the gap value is small enough owing to the lattice mismatch. However, it can be increased by applying a perpendicular electric field [30].

Creation of various graphene heterostructures, including SLs, with the gap discontinuity is widely discussed now. One way of generating spatially modulated gap is graphene on a substrate made from different dielectrics [31]. The required gap modulation can also be created by using, e.g., an inhomogeneously hydrogenated graphene or graphene sheet with nonuniformly deposited CrO_3 molecules. In our previous work [32] we studied the electronic properties of graphene SL in which the gap and potential profile are piecewise constant functions. It was found that in such a SL up to some critical value V_c of potential allowed subbands are separated by gaps. When the potential value is greater than or equal to V_c the contact or cone-like Dirac points appear in the spectrum. As a result, SL becomes gapless.

In this work we examine in detail ballistic transport through graphene nanostructures, including SL, formed by space-modulated gap and potential. Using the transfer-matrix formalism we study the transmission, conductance and the Fano factor for systems with an arbitrary numbers of barriers.

2. Basic equations

Let us initially consider a lateral one-dimensional multibarrier structure consisting of N strips with widths d_j ($j=1,\ldots,N$) characterized by the gaps Δ_j and potential heights V_j (see Fig. 1). The outer regions labeled by 0 and $N+1$ correspond to the gapless graphene with $\Delta=V=0$. In jth strip, the carriers are described by the two-dimensional Dirac equation

$$(\hbar v_F \boldsymbol{\sigma}\mathbf{k}+\Delta_j\sigma_z)\Psi_j=(E-V_j)\Psi_j, \tag{1}$$

where $\hbar\mathbf{k}$ is the momentum operator, $\boldsymbol{\sigma}$ is the vector of Pauli matrices, and $v_F\approx 10^6$ m/s is the Fermi velocity. Due to translation

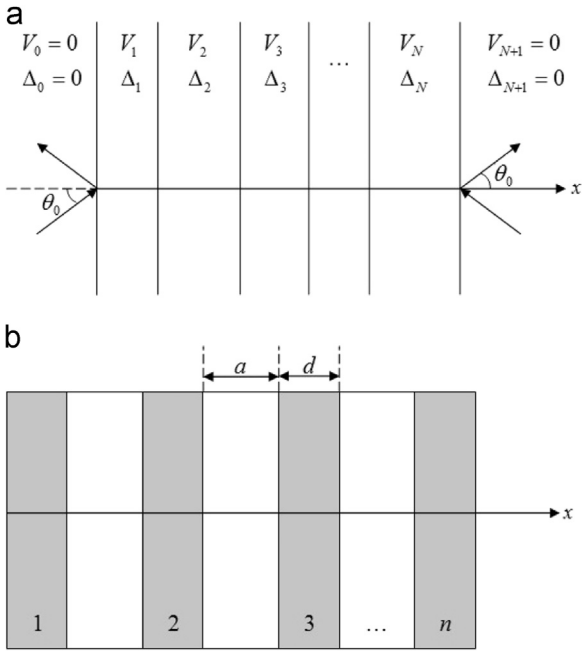

Fig. 1. (a) Model of graphene structure represented by series slabs of width d_j ($j=1,\ldots,N$) characterized by gaps Δ_j and potential V_j. (b) Schematic diagram of a Kronig–Penney type multibarrier structure, in which the gap and potential equal to Δ and V, respectively, in the gray regions and zero outside.

invariance in the y-direction, the solution of Eq. (1) in the jth region can be written as $\Psi_j(x,y)=\Psi_j(x)\exp(ik_y y)$. It is convenient to define the wavevector k_j as

$$k_j=\frac{\sqrt{(E-V_j)^2-\Delta_j^2}}{\hbar v_F}. \tag{2}$$

Then for $k_j^2>k_y^2$ the wavefunction $\Psi_j(x)$ in strip j ($x_j^L\le x\le x_j^R$) is a superposition of plane waves

$$\Psi_j(x)=\frac{A_j}{\sqrt{\delta_j^2+1}}\begin{pmatrix}1\\ \sigma_j\delta_j e^{i\theta_j}\end{pmatrix}\exp(ik_j x\cos\theta_j) + \frac{B_j}{\sqrt{\delta_j^2+1}}\begin{pmatrix}1\\ -\sigma_j\delta_j e^{-i\theta_j}\end{pmatrix}\exp(-ik_j x\cos\theta_j). \tag{3}$$

Here, $\theta_j=\tan^{-1}(k_y/k_{xj})$, $k_{xj}=\sqrt{(E-V_j)^2-\Delta_j^2-(\hbar v_F k_y)^2}/\hbar v_F$, $\theta_j\in[-\pi/2,\pi/2]$, $\delta_j=\sqrt{(E-V_j-\Delta_j)/(E-V_j+\Delta_j)}$, $\sigma_j=\mathrm{sgn}(E-V_j+\Delta_j)$. x_j^L and x_j^R denote the left and right boundaries of the strip j, respectively, so that $x_{j-1}^R=x_j^L$. In the opposite case, when $k_j^2<k_y^2$, solution $\Psi_j(x)$ has pure exponential behavior along the x-axis.

Suppose that $\Psi_j(x)$ oscillates everywhere. Then we define the functions $A_j(x)=A_j\exp(ik_j x\cos\theta_j)$, $B_j(x)=B_j\exp(-ik_j x\cos\theta_j)$. As a result, Eq. (3) may be written in the form

$$\Psi_j(x)=L_j\begin{pmatrix}A_j(x)\\ B_j(x)\end{pmatrix}, \tag{4}$$

where

$$L_j=\frac{1}{\sqrt{\delta_j^2+1}}\begin{pmatrix}1 & 1\\ \sigma_j\delta_j e^{i\theta_j} & -\sigma_j\delta_j e^{-i\theta_j}\end{pmatrix}. \tag{5}$$

Continuity of the upper and lower components $\Psi_j(x)$ at the strip boundaries requires that

$$L_{j-1}\begin{pmatrix}A_{j-1}^R\\ B_{j-1}^R\end{pmatrix}=L_j\begin{pmatrix}A_j^L\\ B_j^L\end{pmatrix}. \tag{6}$$

Within the region j the solutions (A_j^L, B_j^L) and (A_j^R, B_j^R) are connected by the free propagation matrix K_j:

$$\begin{pmatrix}A_j^R\\ B_j^R\end{pmatrix}=K_j\begin{pmatrix}A_j^L\\ B_j^L\end{pmatrix}, \tag{7}$$

where

$$K_j=\begin{pmatrix}e^{ik_j d_j\cos\theta_j} & 0\\ 0 & e^{-ik_j d_j\cos\theta_j}\end{pmatrix}. \tag{8}$$

Combining Eqs. (7) and (8) one can find

$$\begin{pmatrix}A_{N+1}^L\\ B_{N+1}^L\end{pmatrix}=M\begin{pmatrix}A_0^R\\ B_0^R\end{pmatrix}, \tag{9}$$

where the transfer matrix M is introduced for the considered heterostructure as

$$M=L_{N+1}^{-1}F_N F_{N-1}\ldots F_1 L_0. \tag{10}$$

Here $L_{N+1}=L_0$ is determined by Eq. (5) at $V=\Delta=0$ and $F_j=L_j K_j L_j^{-1}$, which yields

$$F_j=\frac{1}{\cos\theta_j}\begin{pmatrix}\cos(k_j d_j\cos\theta_j-\theta_j) & \frac{i\sigma_j}{\delta_j}\sin(k_j d_j\cos\theta_j)\\ i\sigma_j\delta_j\sin(k_j d_j\cos\theta_j) & \cos(k_j d_j\cos\theta_j+\theta_j)\end{pmatrix}. \tag{11}$$

We may use Eq. (11) for an arbitrary multibarrier structure, characterized by different parameters Δ_j and V_j in each slab of width d_j.